Correspondence

Diversity Analysis of Coded Spatial Multiplexing MIMO AF Relaying Systems

Minki Ahn, *Student Member, IEEE*, Changick Song, *Member, IEEE*, and Inkyu Lee, *Senior Member, IEEE*

***Abstract*—In this paper, we analyze the diversity performance of source–relay joint precoding in spatial multiplexing (SM) multiple-input–multiple-output (MIMO) amplify-and-forward (AF) relaying systems with channel coding. First, we evaluate the achievable diversity order of singular-value-decomposition-based precoding schemes as a function of a code rate. Then, we show that a significant diversity improvement can be obtained by utilizing signal space diversity. Our analysis provides helpful insights on the tradeoff between the code rate and the diversity order in SM MIMO AF relaying systems. Simulation results demonstrate that our analytical expressions match well with the numerical results.**

***Index Terms*—Channel coded systems, diversity, multiple-input–multiple-output (MIMO), relay.**

I. Introduction

In recent years, wireless relaying systems combined with multiple-input–multiple-output (MIMO) techniques have attracted much attention due to its ability of coverage extension and spectral efficiency improvement. Several relay protocols have been developed such as amplify-and-forward (AF) and decode-and-forward (DF) protocols [1]. Compared with the DF, the AF protocol is more suitable for practical systems due to its simple implementation and low power consumption as a result of retransmission without the decoding procedure. Thus, in this paper, we focus on the AF relaying systems.

Considering spatial multiplexing (SM) transmission in MIMO AF relaying systems that transmit multiple data streams simultaneously, many source–relay joint precoding schemes have been recently proposed based on the minimum mean square error (MMSE) criterion [2]. Many works have been also carried out to characterize the analytical performance of MIMO AF relaying systems in (see [3]–[5] and references therein). Specifically, the average bit-error-rate (BER) performance of a single stream beamforming scheme was analyzed in [3]. Extending this to the case of the SM, the authors in [4] investigated the average BER performance of joint precoding methods in terms of a diversity gain. However, all these works are mostly limited to uncoded systems. In fact, channel coding is employed in most practical communication systems to improve the link reliability. Nevertheless, relatively few efforts have been devoted to analyzing coded SM MIMO relaying systems.

Manuscript received April 8, 2013; revised September 24, 2013 and November 26, 2013; accepted November 29, 2013. Date of publication December 11, 2013; date of current version September 11, 2014. This work was supported by the National Research Foundation of Korea funded by the Korean government (Ministry of Education, Science and Technology) under Grant 2010-0017909. The review of this paper was coordinated by Prof. W. A. Krzymien.

M. Ahn and I. Lee are with the School of Electrical Engineering, Korea University, Seoul 136-701, Korea (e-mail: amk200@korea.ac.kr; inkyu@korea.ac.kr).

C. Song is with the Department of Electrical and Electronic Engineering, Imperial College, London SW7 2AZ, U.K. (e-mail: csong@imperial.ac.uk).

Color versions of one or more of the figures in this paper are available online at http://ieeexplore.ieee.org.

Digital Object Identifier 10.1109/TVT.2013.2294648

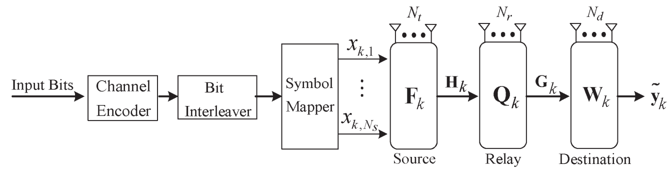

Fig. 1. System description for coded SM MIMO AF relaying systems.

In this paper, we first analyze the achievable diversity order of conventional singular value decomposition (SVD)-based source–relay precoding systems with channel coding by means of the error covariance matrix decomposition technique. Then, a tradeoff between the code rate and the diversity order is characterized. From this tradeoff, it is shown that with a high code rate, the error performance of the SVD-based precoding scheme suffers from low diversity gains. From the observation in the decomposed error covariance matrix structure, we can see that the signal space diversity (SSD) techniques in [6] can improve the diversity gain. Hence, the SSD-based precoding method is applied to the coded SM relaying systems and analyzes its diversity order. Then, the SSD-based precoding scheme outperforms the SVD-based precoding scheme in terms of diversity gain for the same code rate. Finally, simulation results will be presented to confirm the accuracy of our diversity analysis.

Throughout this paper, we use the following notations. Normal letters represent scalar quantities, boldface lowercase letters indicate vectors, and boldface uppercase letters designate matrices. In addition, $\{\cdot\}^T$, $\{\cdot\}^H$, $\mathbb{E}[\cdot]$, and tr$(\cdot)$ stand for transpose, conjugate transpose, expectation, and trace, respectively. The Euclidean norm of a vector $\mathbf{x}$ is denoted by $\|\mathbf{x}\|$. In addition, diag$\{x_1, \ldots, x_K\}$ and blkdiag$\{\mathbf{X}_1, \ldots, \mathbf{X}_K\}$ represent a diagonal matrix and a block diagonal matrix, respectively.

II. System Model

We consider coded SM MIMO AF relaying systems, as shown in Fig. 1. The relaying system is equipped with N_t source, N_r relay, and N_d destination antennas, where $N_s \leq \min\{N_t, N_r, N_d\}$ independent data streams are simultaneously transmitted. We assume that a direct link between the source and the destination is ignored due to a large path loss. In addition, the relay node is assumed to operate in a half-duplex mode. A single-channel encoder followed by a bit interleaver is employed at the source to support all substreams. In this case, consecutive coded bits can be randomly interleaved in each substream such that only 1-bit error occurs in each symbol.

The signal transmission from the source to the destination is carried out in two stages. In the first stage, the information bits are encoded with the code rate R_c and modulated by the symbol mapper. Then, the kth time-modulated symbol vector is given by $\mathbf{x}_k \in \mathbb{C}^{N_s \times 1}$ with $\mathbb{E}[\mathbf{x}_k\mathbf{x}_k^H] = \sigma_x^2\mathbf{I}_{N_s}$ for $k = 1, 2, \ldots, L$ with the frame size L. The signal vector $\mathbf{x}_k$ is precoded by the precoding matrix $\mathbf{F}_k \in \mathbb{C}^{N_t \times N_s}$ and then transmitted to the relay. Assuming tr$(\mathbf{F}_k\mathbf{F}_k^H) = N_s$, we define the source transmit power as $P_T = \mathbb{E}[\|\mathbf{F}_k\mathbf{x}_k\|^2] = \sigma_x^2 N_s$. Then, the received signal $\mathbf{y}_k$ at the relay is given by $\mathbf{y}_k = \mathbf{H}_k\mathbf{F}_k\mathbf{x}_k + \mathbf{n}_k$, where $\mathbf{H}_k \in \mathbb{C}^{N_r \times N_t}$ denotes the first-hop channel matrix and $\mathbf{n}_k$ represents the complex Gaussian noise vector with zero mean and unit variance at the relay.

In the second stage, the relay signal $\mathbf{y}_k$ is precoded by the relay filter $\mathbf{Q}_k \in \mathbb{C}^{N_r \times N_r}$, where $\mathbf{Q}_k$ satisfies the relay transmit power P_R as $\mathbb{E}[\|\mathbf{Q}_k\mathbf{y}_k\|^2] = P_R$. Finally, the received signal at the destination is written by

$$\begin{aligned}\tilde{\mathbf{y}}_k &= \mathbf{W}_k(\mathbf{G}_k\mathbf{Q}_k\mathbf{y}_k + \mathbf{z}_k)\\ &= \mathbf{W}_k\mathbf{G}_k\mathbf{Q}_k\mathbf{H}_k\mathbf{F}_k\mathbf{x}_k + \mathbf{W}_k\mathbf{G}_k\mathbf{Q}_k\mathbf{n}_k + \mathbf{W}_k\mathbf{z}_k \end{aligned} \tag{1}$$

where $\mathbf{z}_k$ designates the complex Gaussian noise vector with zero mean and unit variance at the destination, $\mathbf{G}_k \in \mathbb{C}^{N_d \times N_r}$ stands for the second-hop channel matrix, and $\mathbf{W}_k \in \mathbb{C}^{N_s \times N_d}$ indicates the linear receiver at the destination. In this paper, we assume Rayleigh block-fading MIMO channels with antenna correlation at the destination.[1] Then, the second-hop channel matrix $\mathbf{G}_k$ can be described as $\mathbf{G}_k = \mathbf{\Sigma}^{(1/2)}\tilde{\mathbf{G}}_k$, where $\mathbf{\Sigma} = (\mathbf{\Sigma}^{(1/2)})(\mathbf{\Sigma}^{(1/2)})^H$ is the correlation matrix. The channel matrices $\mathbf{H}_k$ and $\tilde{\mathbf{G}}_k$ have independent and identically distributed zero-mean complex Gaussian entries with unit variance and do not change within a frame.

III. Diversity Analysis of Singular Value Decomposition-Based Joint Precoding Schemes

Here, we present the pairwise error probability (PEP) analysis for SVD-based joint source–relay precoding (SVD-JP) schemes in [2], whose performance is shown to be optimal in terms of mean square error at high signal-to-noise ratio (SNR). The authors in [2] have shown that the relay transceiver $\mathbf{Q}_k$ can be decomposed as $\mathbf{Q}_k = \mathbf{B}_k\mathbf{L}_k$, where $\mathbf{L}_k \in \mathbb{C}^{N_s \times N_r}$ denotes the MMSE receiver for the first-hop channel and $\mathbf{B}_k \in \mathbb{C}^{N_r \times N_s}$ is a matrix that is referred to as the relay precoder. In addition, the optimal receiver $\mathbf{W}_k$ is easily calculated as the Wiener filter.

Then, for a given structure of $\mathbf{L}_k$ and $\mathbf{W}_k$, the error covariance matrix $\mathbf{R}_e \triangleq \mathbb{E}[(\tilde{\mathbf{y}}_k - \mathbf{x}_k)(\tilde{\mathbf{y}}_k - \mathbf{x}_k)^H]$ can be written at high SNR as

$$\mathbf{R}_e = \mathbf{R}_h + \mathbf{R}_g \tag{2}$$

where $\mathbf{R}_h \triangleq (\mathbf{F}_k^H\mathbf{H}_k^H\mathbf{H}_k\mathbf{F}_k + \sigma_x^{-2}\mathbf{I}_{N_s})^{-1}$, and $\mathbf{R}_g \triangleq (\mathbf{B}_k^H\mathbf{G}_k^H\mathbf{G}_k\mathbf{B}_k + \sigma_x^{-2}\mathbf{I}_{N_s})^{-1}$. In this case, the optimal precoders for both $\mathbf{F}_k$ and $\mathbf{B}_k$ are generally given by $\mathbf{F}_k = \mathbf{V}_h\Delta_h$ and $\mathbf{B}_k = \mathbf{V}_g\Delta_g$, where $\mathbf{V}_h$ and $\mathbf{V}_g$ are constructed by the first N_s columns of the right singular matrix of $\mathbf{H}_k$ and $\mathbf{G}_k$, respectively, and Δ_h and Δ_g are the diagonal power loading matrices. In this paper, we assume $\Delta_h = \Delta_g = \mathbf{I}$ for simplicity since the power loading does not affect the diversity order [7].

Applying the SVD-JP scheme, the received signal in (1) can be rewritten by $\tilde{\mathbf{y}}_k = \mathbf{x}_k + \tilde{\mathbf{n}}_k$, where the effective noise $\tilde{\mathbf{n}}_k$ is defined by $\tilde{\mathbf{n}}_k = \mathbf{W}_k\mathbf{G}_k\mathbf{Q}_k\mathbf{n}_k + \mathbf{W}_k\mathbf{z}_k$ with the covariance matrix $\mathbf{R}_e$ in (2). Then, a maximum-likelihood (ML) decoder at the destination makes a decision according to the rule as

$$\begin{aligned}\bar{\mathbf{c}} &= \arg\min_{\mathbf{c}\in\mathcal{C}} \sum_{k=1}^{L} \left\| \mathbf{R}_e^{-\frac{1}{2}}(\tilde{\mathbf{y}}_k - \mathbf{x}_k)\right\|^2\\ &= \arg\min_{\mathbf{c}\in\mathcal{C}} \sum_{k=1}^{L}\sum_{i=1}^{N_s} \frac{|\tilde{y}_{k,i} - x_{k,i}|^2}{\sigma_i^2}\end{aligned}$$

where $\mathcal{C}$ denotes a codebook, and σ_i^2 represents the ith diagonal element of $\mathbf{R}_e$. Here, σ_i^2 can be approximated at high SNR as $\sigma_i^2 \approx \lambda_{h,i}^{-1} + \lambda_{g,i}^{-1}$ [8], where $\lambda_{h,i}$ and $\lambda_{g,i}$ are equal to the ith largest eigenvalue of $\mathbf{H}_k^H\mathbf{H}_k$ and $\mathbf{G}_k^H\mathbf{G}_k$, respectively.

Now, we consider the conditional PEP that an ML decoder chooses the erroneous coded bit sequence $\bar{\mathbf{c}}$ over the transmitted coded bit sequence $\mathbf{c}$. Assuming that $\bar{\mathbf{x}}_k$ and $\mathbf{x}_k$ correspond to the symbol sequence associated with the coded bit sequence $\bar{\mathbf{c}}$ and $\mathbf{c}$, respectively, the PEP given $\mathbf{H}_k$ and $\mathbf{G}_k$ is expressed by

$$\begin{aligned}&P\{\mathbf{c} \to \bar{\mathbf{c}} | \mathbf{H}_k, \mathbf{G}_k, \forall k\}\\ &= P\left\{ \sum_{k=1}^{L}\sum_{i=1}^{N_s} \frac{(|\tilde{y}_{k,i} - x_{k,i}|^2 - |\tilde{y}_{k,i} - \bar{x}_{k,i}|^2)}{\sigma_i^2} > 0 \right\}\\ &= Q\left(\sqrt{\frac{\sigma_x^2}{2}\sum_{k=1}^{L}\sum_{i=1}^{N_s} \frac{\lambda_{h,i}\lambda_{g,i}}{\lambda_{h,i}+\lambda_{g,i}} \frac{(x_{k,i} - \bar{x}_{k,i})^2}{\sigma_x^2}} \right)\\ &\le \exp\left(-\frac{\sigma_x^2}{4}\sum_{i=1}^{N_s} \mu_i d_{E,i}\right)\end{aligned} \tag{3}$$

where $d_{E,i} \triangleq \sum_{k=1}^{L}(x_{k,i} - \bar{x}_{k,i})^2/\sigma_x^2$ indicates the sum of the normalized Euclidean distance, and $\mu_i \triangleq \lambda_{h,i}\lambda_{g,i}/(\lambda_{h,i} + \lambda_{g,i})$ is defined as the ith substream channel gain. Note that the Chernoff bound in (3) is tight at high SNR in terms of diversity gain. Then, averaging the exponential function in (3) with respect to $\mathbf{H}_k$ and $\mathbf{G}_k$ for all k, we obtain the achievable diversity order of the SVD-JP scheme as summarized in the following theorem.

Theorem 1: For the SVD-JP scheme of coded MIMO AF relaying systems with a code rate R_c, the achievable diversity order is obtained by

$$\begin{aligned}D_{\mathrm{SVD-JP}} &= (N_r - \lceil R_c \cdot N_s\rceil + 1)\\ &\quad\times (\min(N_t, N_d) - \lceil R_c \cdot N_s \rceil + 1)\end{aligned} \tag{4}$$

where $\lceil x \rceil$ is equal to the smallest integer value not less than x.

Proof: See Appendix A.

Our analytical result provides valuable insights on the relation between the code rate and the diversity order of AF relaying systems that transmit multiple data streams. We can see from Theorem 1 that the result includes existing works for uncoded systems as a special case. For example, the diversity order of uncoded relaying systems ($R_c = 1$) is determined by $(N_r - N_s + 1)(\min(N_t, N_d) - N_s + 1)$, which is given in [4].

Through the derived diversity order in (4), we can choose the proper code rate to achieve a desired diversity order for given system configurations. For example, if we set the code rate R_c less than or equal to $1/N_s$, a full diversity order $N_r \cdot \min(N_t, N_d)$ [4] is always achievable. In contrast, when a high rate code is employed to support high spectral efficiency, the diversity performance of the coded SVD-JP scheme may seriously deteriorate. In the next section, we introduce a precoding scheme based on the SSD in [6], which provides a significant performance improvement compared with the conventional SVD-JP scheme and analyze its diversity order.

IV. Diversity Analysis of the Signal Space Diversity-Based Joint Precoding Scheme

Here, we apply an SSD-based joint source–relay precoding (SSD-JP) scheme to SM AF relaying systems and analyze its diversity order assuming the channel encoder at the source. Then, we show that it achieves a significant diversity advantage over the conventional

[1] In practical systems, antenna correlation occurs since mobile user's antennas are placed close to each other due to space limitation.

SVD-JP scheme. Applying the SSD-based precoding technique, the precoding matrices of the source and the relay are obtained as

$$\tilde{\mathbf{F}}_k = \tilde{\mathbf{V}}_h \mathbf{P}_1 \text{ and } \tilde{\mathbf{B}}_k = \tilde{\mathbf{V}}_g \mathbf{P}_2$$

where we define $\tilde{\mathbf{V}}_h$ and $\tilde{\mathbf{V}}_g$ as the reordered matrices of $\mathbf{V}_h$ and $\mathbf{V}_g$, i.e., $\tilde{\mathbf{V}}_h \triangleq [\mathbf{v}_{h,1}\mathbf{v}_{h,N_s}\mathbf{v}_{h,2}\mathbf{v}_{h,N_s-1}\cdots\mathbf{v}_{h,N_s/2}\mathbf{v}_{h,N_s/2+1}]$ and $\tilde{\mathbf{V}}_g \triangleq [\mathbf{v}_{g,1}\mathbf{v}_{g,N_s}\mathbf{v}_{g,2}\mathbf{v}_{g,N_s-1}\cdots\mathbf{v}_{g,N_s/2}\mathbf{v}_{g,N_s/2+1}]$, respectively, and the rotation matrices $\mathbf{P}_j = \text{blkdiag}\{\mathbf{\Omega}_j, \mathbf{\Omega}_j, \ldots, \mathbf{\Omega}_j\}$ for $j \in \{1, 2\}$ consist of the 2×2 unitary matrix $\mathbf{\Omega}_j = \begin{bmatrix} \alpha_j & \beta_j \\ -\beta_j & \alpha_j \end{bmatrix}$ with the fixed α_j and β_j given in [6].

Since the substream channel gains are combined by the precoding matrix $\mathbf{\Omega}_j$, the worst effective channel gain of the paired substreams can be higher than that of the substream channel gains in the SVD-JP scheme. The decomposed error covariance matrix in (2) can be expressed as a block diagonal matrix when an identical rotation matrix $\mathbf{P}_1 = \mathbf{P}_2 = \mathbf{P}$ (i.e., $\mathbf{\Omega}_1 = \mathbf{\Omega}_2 = \mathbf{\Omega}$) is employed at the precoding matrices of the source and the relay.

Then, the error covariance matrix is rewritten as

$$\begin{aligned}\tilde{\mathbf{R}}_e &= \left(\tilde{\mathbf{F}}_k^H \mathbf{H}_k^H \mathbf{H}_k \tilde{\mathbf{F}}_k + \sigma_x^{-2}\mathbf{I}_{N_s}\right)^{-1} \\ &\quad + \left(\tilde{\mathbf{B}}_k^H \mathbf{G}_k^H \mathbf{G}_k \tilde{\mathbf{B}}_k + \sigma_x^{-2}\mathbf{I}_{N_s}\right)^{-1} \\ &= \mathbf{P}^H \mathbf{R}_e \mathbf{P} \\ &= \text{blkdiag}\left\{\tilde{\mathbf{R}}_{e,1}, \ldots, \tilde{\mathbf{R}}_{e,N_s/2}\right\} \qquad (5)\end{aligned}$$

where $\tilde{\mathbf{R}}_{e,i}$ is defined by $\tilde{\mathbf{R}}_{e,i} \triangleq \mathbf{\Omega}^H \mathbf{R}_{e,i} \mathbf{\Omega}$. Here, $\mathbf{R}_{e,i}$ denotes the ith 2×2 subblock matrix of $\mathbf{R}_e = \text{diag}\{\sigma_1^2, \ldots, \sigma_{N_s}^2\}$ in (2). By applying this new error covariance matrix, we can derive the achievable diversity order of the SSD-JP scheme.

Let the received signal at the destination be $\tilde{\mathbf{y}}_k = \mathbf{x}_k + \tilde{\mathbf{z}}_k$, where the effective noise $\tilde{\mathbf{z}}_k$ is defined by $\tilde{\mathbf{z}}_k = \mathbf{W}_k \mathbf{G}_k \mathbf{Q}_k \mathbf{n}_k + \mathbf{W}_k \mathbf{z}_k$ with the covariance matrix $\tilde{\mathbf{R}}_e$. Utilizing the Cholesky decomposition, $\tilde{\mathbf{R}}_{e,i}^{-1}$ can be written by $\mathbf{M}_i^H \mathbf{M}_i$ with $\mathbf{M}_i = \mathbf{R}_{e,i}^{-1/2}\mathbf{\Omega}$, and then the ML decoder at the destination chooses

$$\begin{aligned}\bar{\mathbf{c}} &= \arg\min_{\mathbf{c}\in\mathcal{C}} \sum_{k=1}^{L} \|\mathbf{M}(\tilde{\mathbf{y}}_k - \mathbf{x}_k)\|^2 \\ &= \arg\min_{\mathbf{c}\in\mathcal{C}} \sum_{k=1}^{L} \sum_{i=1}^{N_s/2} \|\mathbf{M}_i(\tilde{\mathbf{y}}_{k,i} - \mathbf{x}_{k,i})\|^2 \qquad (6)\end{aligned}$$

where $\mathbf{M}$, $\tilde{\mathbf{y}}_{k,i}$, and $\mathbf{x}_{k,i}$ are defined as $\mathbf{M} \triangleq \text{blkdiag}\{\mathbf{M}_1, \ldots, \mathbf{M}_{N_s/2}\}$, $\tilde{\mathbf{y}}_{k,i} \triangleq [\tilde{y}_{k,2i-1}\tilde{y}_{k,2i}]^T$, and $\mathbf{x}_{k,i} \triangleq [x_{k,2i-1}x_{k,2i}]^T$, respectively.

Since $\mathbf{M}_i$ is a 2×2 real matrix, the real-valued representation for the aforementioned ith subblock channel matrix in (6) can be equivalently represented as [9]

$$\bar{\mathbf{c}} = \arg\min_{\mathbf{c}\in\mathcal{C}} \sum_{k=1}^{L} \sum_{i=1}^{N_s/2} \sum_{l\in I,Q} \left\|\mathbf{M}_i\left(\tilde{\mathbf{y}}_{k,i}^l - \mathbf{x}_{k,i}^l\right)\right\|^2 \qquad (7)$$

where superscripts I and Q indicate the in-phase and quadrature parts of a complex vector, respectively. Here, the ML decoder in (7) allows a single symbol decodable detection at the destination. In fact, this real-valued representation can be also applied to the SVD-JP scheme, and thereby, it leads to a half-symbol decodable receiver [10]. The complexity of the ML decoder of the SSD-JP scheme is $\sqrt{M}$ times higher than that of the SVD-JP scheme, where M is the modulation level. Consequently, the SSD-JP scheme can provide an additional diversity gain at the expense of the increased receiver complexity. In the following theorem, we present the diversity order of the SSD-JP scheme.

Theorem 2: For the SSD-JP scheme of coded MIMO AF relaying systems with a code rate R_c, the achievable diversity order is obtained by

$$\begin{aligned}D_{\text{SSD-JP}} &= \left(N_r - \left\lceil \frac{R_c \cdot N_s}{2} \right\rceil + 1\right) \\ &\quad \times \left(\min(N_t, N_d) - \left\lceil \frac{R_c \cdot N_s}{2} \right\rceil + 1\right).\end{aligned}$$

Proof: See Appendix B.

From the result in Theorem 2, we can see that the SSD-JP has a diversity advantage over the SVD-JP scheme when $R_c > (1/N_s)$. For example, for the SSD-JP scheme with $N_t = N_r = N_d = N_s = 2$, a full diversity order is guaranteed even in the uncoded system $R_c = 1$, whereas the SVD-JP scheme achieves the full diversity only when $R_c \leq (1/2)$. With this diversity analysis, we demonstrate that the SSD-JP method is indeed efficient in terms of the diversity order in SM MIMO AF relaying systems.

Remark 1: From (10) in Appendix A, we can see that relaying systems with spatially uncorrelated Rayleigh MIMO channels also have the same achievable diversity order since antenna correlation only affects the constant value b_i. Thus, our diversity order results also hold on the spatially uncorrelated Rayleigh MIMO channels, and this will be confirmed through simulation in the following section.

V. Simulation Results

Here, we present Monte Carlo simulations to support the analytical results derived in the previous sections. Throughout this paper, we employ a convolutional encoder [11] with a random bit interleaver. The frame size is set to $L = 64$, and QPSK modulation is used in all simulation. Denoting the total transmit power by P_0, we assume that $P_T = P_R = P_0/2$ for simplicity. Although our analytical results are general and valid for arbitrary correlation matrices $\mathbf{\Sigma}$, we consider the exponential correlation model with $\mathbf{\Sigma} = \{\rho^{|i-j|}\}_{i,j=1,\ldots,N_d}$ and $\rho \in [0, 1)$. The elements of $\mathbf{\Omega}$ in the SSD-JP scheme are set to be $\alpha = 1/\sqrt{1+\tau^2}$ and $\beta = \tau\alpha$, where $\tau = 0.49$.[2] In addition, a diversity order of the average FER slope in figures is denoted by D.

Fig. 2 provides the numerical performance of the SVD-JP and SSD-JP schemes with various code rates for $N_t = N_r = N_d = N_s = 2$. In this case, the full diversity order of this relaying system is equal to 4 from $N_r \min(N_t, N_d)$ [4]. From the uncoded case ($R_c = 1$), we can see that applying channel coding improves the average FER performance. The plots confirm that the SVD-JP scheme with the code rate of 1/2, 3/4, and 1 provides the diversity orders of 4, 1, and 1, respectively, which are the same as the analysis results in (4). In contrast, the curves of the SSD-JP scheme yield the full diversity order of 4 for all code rates. In addition, the diversity orders of uncorrelated Rayleigh fading channels (i.e., $\rho = 0$) are identical to the correlated cases. These results show that antenna correlation does not affect the diversity orders.

Similar observations can be made in Fig. 3, which illustrates the average FER performance of the SVD-JP and SSD-JP scheme in the case of $N_t = N_r = N_d = N_s = 3$. The SSD-JP scheme achieves the full diversity order of 9 in the code rates of 1/2 and 2/3, respectively, whereas the SVD-JP scheme obtains a diversity order of 4 for

[2]Similar to the method in [6], τ is determined through an exhaustive search such that the frame error rate (FER) is minimized.

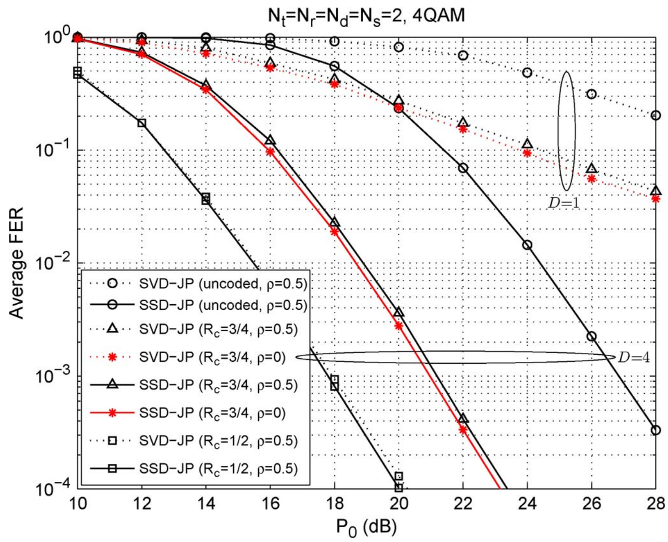

Fig. 2. Average FER performance as a function of the total transmit power P_0 with various code rates.

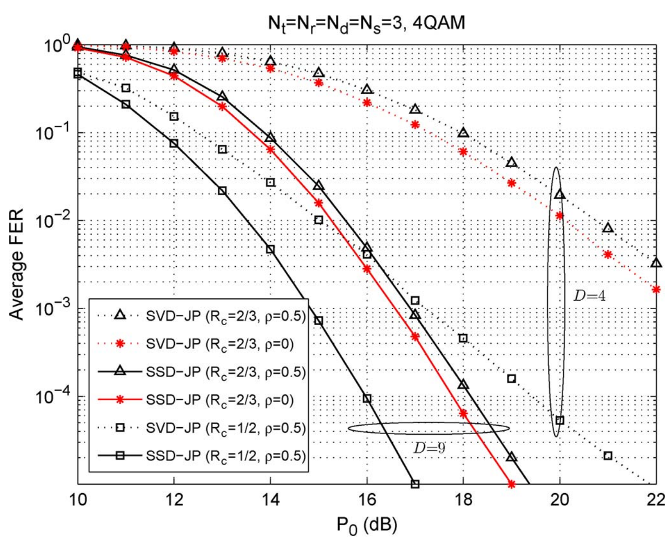

Fig. 3. Average FER performance as a function of the total transmit power P_0 with various code rates.

the same code rates. Then, we see from these figures that the SSD-JP scheme outperforms the SVD-JP scheme in terms of the diversity order. In addition, we confirm that the diversity orders of the average FER slopes in various code rates agree with the derived diversity orders.

VI. Conclusion

In this paper, we have investigated the analytical performance of coded SM MIMO AF relaying systems. First, the achievable diversity order of the SVD-JP scheme has been derived by carrying out the PEP analysis. To improve the error performance, we have examined the SSD-based precoding scheme and analyzed its diversity performance, which obtains a higher diversity order than the SVD-JP scheme for a larger range of code rates. Through the derived analytical results, we gain insights on the relationship between the code rate and the diversity order of coded relaying systems. The simulation results show that our analytic derivations are accurate and match well with the numerical performance.

Appendix A
Proof of Theorem 1

We prove Theorem 1 by showing that both the upper and lower bounds of the PEP in (3) achieve the same diversity order. Let us define p as the maximum number of spatial substreams with zero $d_{E,i}$. When we assume that the worst case for all possible combinations of $\mathbf{c}$ and $\bar{\mathbf{c}}$ has occurred, $d_{E,i}$ becomes zero for $1 \leq i \leq p$ and nonzero for $p+1 \leq i \leq N_s$. Then, we can establish an upper bound and a lower bound as

$$\begin{aligned} d_{E,\max}(N_s-p)\mu_{p+1} &\geq \sum_{i=1}^{N_s} \mu_i d_{E,i} = \sum_{i=p+1}^{N_s} \mu_i d_{E,i} \\ &\geq d_{E,\min} \sum_{i=p+1}^{N_s} \mu_i \geq d_{E,\min}\mu_{p+1} \end{aligned} \tag{8}$$

where $d_{E,\max}$ and $d_{E,\min}$ denote the maximum and the minimum of all nonzero $d_{E,i}$ values, respectively.

First, we consider the lower bound in (8). By applying the harmonic mean inequality $(1/2)\min(a,b) \leq (ab/(a+b)) \leq \min(a,b)$, the conditional PEP in (3) is calculated as

$$\begin{aligned} P\{\mathbf{c} \to \bar{\mathbf{c}} | \mathbf{H}_k, \mathbf{G}_k, \forall k\} &\leq \exp\left(-\frac{\sigma_x^2}{4}\sum_{i=1}^{N_s}\mu_i d_{E,i}\right) \\ &\leq \exp\left(-\frac{\sigma_x^2 d_{E,\min}}{4}\mu_{p+1}\right) \\ &\leq \exp\left(-\frac{\sigma_x^2 d_{E,\min}}{8}w_{p+1}\right) \end{aligned} \tag{9}$$

where $w_i \triangleq \min(\lambda_{h,i}, \lambda_{g,i})$. In the high-SNR regime, the error performance mainly depends on the behavior of w_{p+1} at around zero ($w_{p+1} \to 0^+$). In this case, it is shown in [8] that the probability density function (pdf) of the minimum of two independent random variables is computed as a summation of the pdf of each random variable, i.e., $f_{w_i}(w_i) = f_{\lambda_{h,i}}(w_i) + f_{\lambda_{g,i}}(w_i)$. Here, the eigenvalue distributions of $\mathbf{H}_k^H\mathbf{H}_k$ and $\mathbf{G}_k^H\mathbf{G}_k$ are characterized by complex Wishart matrix distributions with covariance matrices $\mathbf{I}$ and $\mathbf{\Sigma}$, respectively. Employing the ith largest eigenvalue distributions in [12], the $f_{\lambda_{h,i}}(w_i)$ and $f_{\lambda_{g,i}}(w_i)$ at around zero can be expressed as

$$\begin{aligned} f_{\lambda_{h,i}}(w_i) &= a_i w_i^{(N_t-i+1)(N_r-i+1)-1} \\ f_{\lambda_{g,i}}(w_i) &= b_i w_i^{(N_r-i+1)(N_d-i+1)-1} \end{aligned} \tag{10}$$

where the constant values a_i and b_i are given in [12].

From these results, we can calculate the upper bound of the average PEP as

$$\begin{aligned} P\{\mathbf{c} \to \bar{\mathbf{c}}\} &\leq \int_0^\infty \exp\left(-\frac{\sigma_x^2 d_{E,\min}}{8}w_{p+1}\right) f_{w_{p+1}} dw_{p+1} \\ &= \int_0^\infty \exp\left(-\frac{\sigma_x^2 d_{E,\min}}{8}w_{p+1}\right) f_{\lambda_{h,p+1}} dw_{p+1} \\ &\quad + \int_0^\infty \exp\left(-\frac{\sigma_x^2 d_{E,\min}}{8}w_{p+1}\right) f_{\lambda_{g,p+1}} dw_{p+1} \end{aligned}$$

$$= a_{p+1}\left(\frac{\sigma_x^2 d_{E,\min}}{8}\right)^{-(N_t-p)(N_r-p)} + b_{p+1}\left(\frac{\sigma_x^2 d_{E,\min}}{8}\right)^{-(N_r-p)(N_d-p)}. \quad (11)$$

Note that the exact relationship between the code rate R_c and p was shown in [11] as

$$p = \lceil R_c \cdot N_s \rceil - 1. \quad (12)$$

By substituting (12) into (11), the diversity order of the upper bound of the PEP is determined by $(N_r - \lceil R_c \cdot N_s \rceil + 1)(\min(N_t, N_d) - \lceil R_c \cdot N_s \rceil + 1)$. In addition, it is easy to show that the lower bound of the PEP can be obtained from (8) in a similar fashion, and thus, details are omitted. Since the lower bound of the PEP exhibits the same diversity order, the proof is completed. ■

Appendix B
Proof of Theorem 2

Employing a similar approach in Appendix A, the conditional PEP derived from the ML equation (7) is given as

$$\begin{aligned}
&P\{\mathbf{c} \to \bar{\mathbf{c}} | \mathbf{H}_k, \mathbf{G}_k, \forall k\} \\
&= P\left\{ \sum_{k=1}^{L} \sum_{i=1}^{N_s/2} \sum_{l \in I,Q} \left(\left\| \mathbf{M}_i \left(\left(\tilde{\mathbf{y}}_{k,i}^l - \mathbf{x}_{k,i}^l \right) \right) \right\|^2 - \left\| \mathbf{M}_i \left(\tilde{\mathbf{y}}_{k,i}^l - \bar{\mathbf{x}}_{k,i}^l \right) \right\|^2 \right) > 0 \right\} \\
&= P\left\{ \sum_{k=1}^{L} \sum_{i=1}^{N_s/2} \sum_{l \in I,Q} \left(\mathrm{tr}\left(2\mathbb{R}\left\{ \mathbf{M}_i \mathbf{d}_{k,i}^l \tilde{\mathbf{z}}_{k,i}^H \mathbf{M}_i^H \right\} \right) - \left\| \mathbf{M}_i \mathbf{d}_{k,i}^l \right\|^2 \right) > 0 \right\}
\end{aligned}$$

where $\mathbb{R}\{\cdot\}$, $\mathbf{d}_{k,i}^l$, and $\tilde{\mathbf{z}}_{k,i}$ are defined as a real operator, $\mathbf{d}_{k,i}^l \triangleq \mathbf{x}_{k,i}^l - \bar{\mathbf{x}}_{k,i}^l$, and $\tilde{\mathbf{z}}_{k,i} \triangleq [\tilde{z}_{k,i} \tilde{z}_{k,i+1}]^T$, respectively.

Note that $\mathrm{var}(\mathrm{tr}(\mathbb{R}\{\mathbf{M}_i \mathbf{d}_{k,i}^l \tilde{\mathbf{z}}_{k,i}^H \mathbf{M}_i^H\})) = (1/2)\|\mathbf{M}_i \mathbf{d}_{k,i}^l\|^2$. Using this result, we have

$$P\{\mathbf{c} \to \bar{\mathbf{c}} | \mathbf{H}_k, \mathbf{G}_k, \forall k\} \leq \exp\left(\frac{1}{4} \sum_{k=1}^{L} \sum_{i=1}^{N_s/2} \sum_{l \in \{I,Q\}} \left\| \mathbf{M}_i \mathbf{d}_{k,i}^l \right\|^2 \right).$$

By utilizing the equality

$$\begin{aligned}
\left\| \mathbf{M}_i \mathbf{d}_{k,i}^l \right\|^2 &= \left\| \mathbf{R}_{e,i}^{-1/2} \mathbf{\Omega} \mathbf{d}_{k,i}^l \right\|^2 \\
&= \mu_i \left(\alpha d_{k,2i-1}^l + \beta d_{k,2i}^l \right)^2 \\
&\quad + \mu_{N_s-i+1} \left(\alpha d_{k,2i}^l - \beta d_{k,2i-1}^l \right)^2
\end{aligned}$$

the conditional PEP is represented by

$$P\{\mathbf{c} \to \bar{\mathbf{c}} | \mathbf{H}_k, \mathbf{G}_k, \forall k\} \leq \exp\left(-\frac{\sigma_x^2}{4} \sum_{i=1}^{N_s/2} \left(\mu_i \bar{v}_{E,i} + \mu_{N_s-i+1} \tilde{v}_{E,i} \right) \right)$$

where $\bar{v}_{E,i} \triangleq (1/\sigma_x^2) \sum_{k=1}^{L} \sum_{l \in I,Q} (\alpha d_{k,2i-1}^l + \beta d_{k,2i}^l)^2$, and $\tilde{v}_{E,i} \triangleq (1/\sigma_x^2) \sum_{k=1}^{L} \sum_{l \in I,Q} (\alpha d_{k,2i}^l - \beta d_{k,2i-1}^l)^2$.

Let us define q as the maximum number of paired substreams with zero $\bar{v}_{E,i}$. When we assume that the worst case has occurred, we obtain $\bar{v}_{E,i} = 0$ for $1 \leq i \leq q$. Then, we can express the following bounds:

$$\begin{aligned}
\bar{v}_{E,q+1} \mu_{q+1} &\leq \sum_{i=1}^{N_s/2} \left(\mu_i \bar{v}_{E,i} + \mu_{N_s-i+1} \tilde{v}_{E,i} \right) \\
&\leq (N_s - q) \bar{v}_{E,\max} \mu_{q+1}
\end{aligned}$$

where $\bar{v}_{E,\max}$ denotes the maximum of all $\bar{v}_{E,i}$ and $\tilde{v}_{E,i}$. Utilizing the same lower bound approach in Appendix A, we can derive the PEP bound as

$$P\{\mathbf{c} \to \bar{\mathbf{c}}\} \leq a_{q+1} \left(\frac{\sigma_x^2 \bar{v}_{E,q+1}}{4} \right)^{-(N_t-q)(N_r-q)} + b_{q+1} \left(\frac{\sigma_x^2 \bar{v}_{E,q+1}}{4} \right)^{-(N_r-q)(N_d-q)}.$$

From the relationship between the code rate R_c and the paired substreams $q = \lceil R_c \cdot (N_s/2) \rceil - 1$ in [11], the diversity order of the upper bound of the PEP is determined by $(N_r - \lceil R_c \cdot (N_s/2) \rceil + 1)(\min(N_t, N_d) - \lceil R_c \cdot (N_s/2) \rceil + 1)$. The lower bound of the PEP also achieves the same diversity order, and details are omitted. Finally, the proof is completed. ■

References

[1] S. Jin, M. R. McKay, C. Zhong, and K.-K. Wong, "Ergodic capacity analysis of amplify-and-forward MIMO dual-hop systems," *IEEE Trans. Inf. Theory*, vol. 56, no. 5, pp. 2204–2224, May 2010.

[2] C. Song, K.-J. Lee, and I. Lee, "MMSE based transceiver designs in closed-loop non-regenerative MIMO relaying systems," *IEEE Trans. Wireless Commun.*, vol. 9, no. 7, pp. 2310–2319, Jul. 2010.

[3] H. A. S. Raymond, H. Y. Louie, Y. Li, and B. Vucetic, "Performance analysis of beamforming in two hop amplify and forward relay networks with antenna correlation," *IEEE Trans. Wireless Commun.*, vol. 8, no. 6, pp. 3132–3141, Jun. 2009.

[4] C. Song, K.-J. Lee, and I. Lee, "Performance analysis of MMSE-based amplify and forward spatial multiplexing MIMO relaying systems," *IEEE Trans. Commun.*, vol. 59, no. 12, pp. 3452–3462, Dec. 2011.

[5] C. Song, K.-J. Lee, and I. Lee, "MMSE-based MIMO cooperative relaying systems: Closed-form designs and outage behavior," *IEEE J. Sel. Areas Commun.*, vol. 30, no. 8, pp. 1390–1401, Sep. 2012.

[6] J. Boutros and E. Viterbo, "Signal space diversity: A power- and bandwidth-efficient diversity technique for the Rayleigh fading channel," *IEEE Trans. Inf. Theory*, vol. 44, no. 4, pp. 1453–1467, Jul. 1998.

[7] L. G. Ordonez, A. P.-Z. Daniel, P. Palomar, and J. R. Fonollosa, "High-SNR analytical performance of spatial multiplexing MIMO systems with CSI," *IEEE Trans. Signal Process.*, vol. 55, no. 11, pp. 5447–5463, Nov. 2007.

[8] C. Song and I. Lee, "Diversity analysis of coded beamforming in MIMO-OFDM amplify-and-forward Relaying systems," *IEEE Trans. Wireless Commun.*, vol. 10, no. 8, pp. 2445–2450, Aug. 2011.

[9] H. Lee, S. Park, and I. Lee, "Orthogonalized spatial multiplexing for closed-loop MIMO systems," *IEEE Trans. Commun.*, vol. 55, no. 5, pp. 1044–1052, May 2007.

[10] H. Zhao, F. Wang, J. Kuang, W. Wang, and B. Wu, "Precoded MDC-STBC scheme with half-symbol decodable receiver," in *Proc. Commun. Netw. China*, Aug. 2010, pp. 1–6.

[11] K.-J. Lee and I. Lee, "Transceiver design based on blockwise uniform channel decomposition for coded MIMO systems," *IEEE Trans. Wireless Commun.*, vol. 8, no. 8, pp. 4241–4251, Aug. 2009.

[12] L. G. Ordonez, A. P.-Z. Daniel, P. Palomar, and J. R. Fonollosa, "Minimum BER linear MIMO transceivers with adaptive number of substreams," *IEEE Trans. Signal Process.*, vol. 57, no. 6, pp. 2336–2353, Jun. 2009.